NJC

Accepted Manuscript

This is an *Accepted Manuscript*, which has been through the Royal Society of Chemistry peer review process and has been accepted for publication.

Accepted Manuscripts are published online shortly after acceptance, before technical editing, formatting and proof reading. Using this free service, authors can make their results available to the community, in citable form, before we publish the edited article. We will replace this *Accepted Manuscript* with the edited and formatted *Advance Article* as soon as it is available.

You can find more information about *Accepted Manuscripts* in the Information for Authors.

Please note that technical editing may introduce minor changes to the text and/or graphics, which may alter content. The journal's standard Terms & Conditions and the Ethical guidelines still apply. In no event shall the Royal Society of Chemistry be held responsible for any errors or omissions in this *Accepted Manuscript* or any consequences arising from the use of any information it contains.

ROYAL SOCIETY OF CHEMISTRY

www.rsc.org/njc

Mechanism of Claisen rearrangement of allyl phenyl ether from perspective of topological analysis of ELF function.

Sławomir Berski*, Piotr Durlak

Faculty of Chemistry, University of Wrocław, F. Joliot-Curie 14, 50-383, Wrocław Poland.

*Corresponding author:

slawomir.berski@chem.uni.wroc.pl
Url: http://kwanty.wchuwr.pl/?q=berski
Tel:+48713757164; Fax:+ 48713282348

Abstract

The Claisen rearrangement of allyl phenyl ether to 6-(prop-2-en-1-yl) cyclohexa-2,4-dien-1-one has been studied by means of the Bonding Evolution Theory (BET), which combines a topological analysis of electron localization function (ELF) and the catastrophe theory. The reaction can be presented as consisting of 10 main steps separated by fold and cusp catastrophes. The description of the mechanism of the C-O bond breaking is complicated and depends on the DFT method used. It proceeds through a heterolytic cleavage (B3LYP, M052x) with formation of the V_3(O) non-bonding basin in the step II (M052x) or with electron density resonating between the oxygen and carbon atoms in the step II (B3LYP). The C-C bond between the allyl group and the phenol ring is formed after TS in the step VIII. The reaction is terminated by formation of two localized C=C bonds in the phenyl ring in steps IX and X. The localization of $V_{i=1,2}$(C,C) basins - typical for localized double bonds – in the phenyl ring proves a process of the dearomatisation. In the electronic structure of the transition structure distinguishes the non-bonding electron density concentrated in the vicinity of the C2 atom, represented by the V(C2) basin, with 0.28e. This basin is a “bridgehead” for the “construction” of the C-C bond between the phenyl ring and allyl group.

1. Introduction

The Claisen rearrangement is powerful synthetic tool in the organic synthesis [1] and is sometimes described as oxy-variant of the Cope reaction. For the first time it has been reported by Claisen in 1912 for the [3,3] – sigmatropic rearrangement of an allyl aryl ether and allyl vinyl ether [2]. The mechanism of the Claisen rearrangement of the allyl phenyl ether

(APhE) consists of breaking of the carbon – oxygen bond and formation of new carbon – carbon bond. Furthermore, this process is associated with migration of the double C=C bond, formation of the double C=O bond and dearomatisation of an aromatic ring (see Scheme 1).

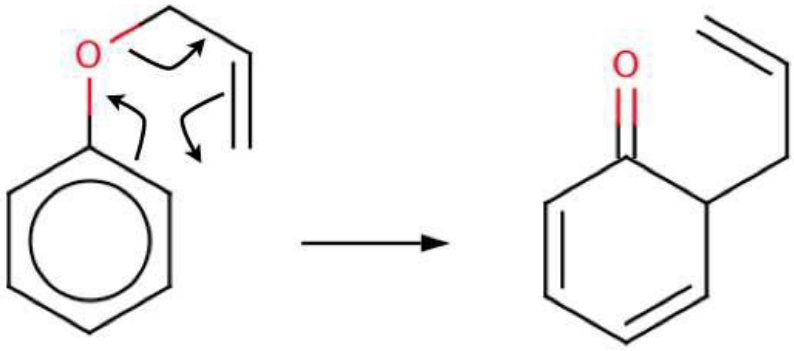

Scheme 1. The Lewis formula for the Claisen rearrangement of allyl phenyl ether to ketonic form of o-allylphenol.

The product of the reaction is the ketonic form of o-allylphenol (KAPh). Finally, a molecule of o-allylphenol, is formed.

The mechanism of the Claisen rearrangement of allyl phenyl ether is usually represented by the Lewis formula with curly arrows showing movements of (formal) electron pairs. However, such mechanism seems to be oversimplified because a few rather fundamental questions may be raised: **1)** Why does the electron density from the delocalised C---C bond of a phenyl ring flow only to the C-O bond (it will be transformed into double C=O bond) and not to both C-O and C---C regions? **2)** Is the mechanism of the Claisen rearrangement of allyl phenyl ether concerted and synchronous i.e. C=O and C-C bonds are formed simultaneously with a breaking of the C-O bond? **3)** In which moment of the reaction are two localized C=C bonds of the phenyl ring formed from previously delocalized C---C bonds? Those and other questions may be answered by using topological analysis of Electron Localization Function (ELF) [3–8] and elements of catastrophe theory [9]. Mechanisms of different organic reactions have been explained using both methods [10–13] and their joined using is known in scientific literature as Bonding Evolution Theory (BET) [14] and was elaborated by Krokidis *et al.* [15–17].

In the past, many theoretical affords have been undertaken to elucidate a nature and a geometry of the transition structure (TS), that is important for understanding the Claisen rearrangements and is believed to be concerted and a chairlike [18]. From the point of view of an organic reactivity, the TS may be considered in terms of the early structure versus its late

character and the 1,4-diyl versus aromatic transformation versus bis-allyl character [19–22]. The geometrical structures of the TS have been analyzed by using AM1, MP2/6-31G(d), RHF/6-31G(d), Becke3LYP/6-31G(d), 6-311+G(d,p) and CASSCF/6-31G(d) computational methods [23].

In this study, a mechanism of the Claisen rearrangement of allyl phenyl ether is studied by means of BET. Our goal is to show the mechanism of reaction as a sequence of a bond breaking and a bond formation that are precisely located on the reaction path by means of catastrophe theory. Furthermore, we want to answer the questions raised above and compare the typical scheme of a flow of electron density with that obtained on basis of ELF–topological study. Though, the Claisen rearrangement of APhE is terminated by formation the o-allylphenol, we have constrained our study to first reaction where ketonic form of the o-allylphenol is formed.

2. Computational details

Optimizations of geometrical structures and calculation of the internal reaction coordinate (IRC) path were performed with Gaussian 03 [24] using the B3LYP [25–28] hybrid electron density functional and 6-31G(d) basis set [29–40] as referenced in the G03 program and M052x global hybrid functional [41] from family of Minnesota functionals as referenced in the Gaussian 09 program [42]. The probing of the IRC path using different DFT functionals encountered many problems therefore standard the B3LYP and M052x functionals have been chosen. The DFT (M052x) method with the 6-311G(d) [43] basis set has been used only to study the reaction path from TS to APhE.

All stationary points were characterized to have the correct type of vibrational eigenvalues, and transition structure was verified to connect to the correct minima by using the IRC method [44,45]. The zero-point vibrational energy of the TS has been calculated by ignoring one imaginary frequency.

For the BET analysis a reaction path was taken from an IRC calculation in mass-weighted Cartesian coordinates with the step length of 0.01 $(amu)^{1/2}$ bohr. The points on the IRC were not interpolated by any specific equation and the line in Figure 3 is presented to emphasize a trend.

The ELF topological analysis was performed by using the TopMod [46] program with the rectangular parallelepipedic grid and the step size of 0.05 bohr. A visualization of molecular structures was done with ChemCraft [47].

The analysis of evolution of the critical points (CPs) is constrained only to attractors localized in the field of the ELF.

The discussion of the points on the IRC path and corresponding interatomic distances, where the process of the A-B bond formation begins and ends is based on the catastrophes of the ELF field. The catastrophe that causes a creation of the non-bonding V(A) or V(B) attractor shows beginning of the bond formation and the catastrophe that causes appearance of the V(A,B) bonding attractor shows the end of bond formation. Those catastrophes have been described for the first time by Krokidis *et al.* [14,15] for the C-C and N-B bond breaking in the C_2H_6 and NH_3BH_3 molecules.

3. Results and discussion

3a. Electronic structure of isolated molecules and transition state

The geometrical structure of the allyl phenyl ether, the ketonic form of the o-allylphenol, and the transition state (TS) of the Claisen rearrangement (see Figure 1) have been optimized at the B3LYP/6-31G(d) computational level.

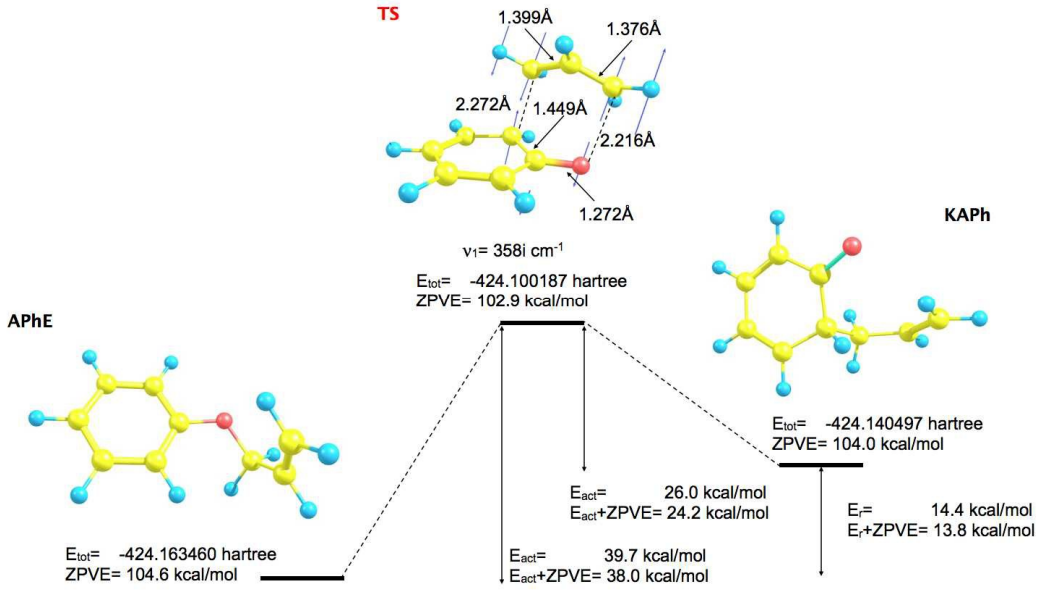

Figure 1. The optimized geometrical structures of minima and transition structure (TS) for the Claisen rearrangement of allyl phenyl ether (APhE).

The predicted activation barrier is 39.7 kcal/mol (36.5 kcal/mol in ref. 48) and 38.0 kcal/mol including zero-point vibrational energy (ZPVE).

The reaction begins from the APhE molecule therefore its electronic structure will be analyzed as a first. The electron densities associated with core regions, covalent bonds and lone pairs are characterized by the local maxima of ELF field (attractors). All attractors localized in APhE are presented in Figure 2.

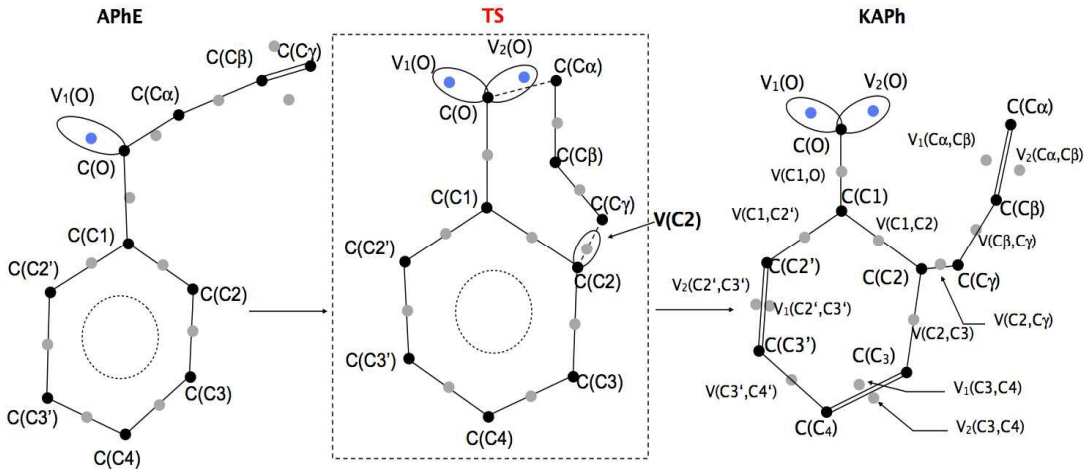

Figure 2. Valence (monosynaptic, disynaptic) and core (monosynaptic) attractors of the ELF field localized for the minima (APhE, KAPh) and transition structure (TS) for the Claisen rearrangement of allyl phenyl ether. The protonated attractors have been omitted for clarity.

The protonated attractors corresponding to H atoms are omitted for clarity. The values of the mean electron population ($\overline{N}$) calculated for each basin of attractor are collected in Table 1.

Table 1. Population (in e) of the ELF-localization basins for different steps in the Claisen rearrangement of allyl phenyl ether (APhE). The first point (after catastrophe) in each domain of structural stability (step of the reaction) is presented.

Basins \ Step	I APhE	IIa IIb	III	IV	V	V TS	VI	VII	VIII	IX	X	X KAPh
r(O···Cα) [Å]	1.422	1.873 [1)]	1.893	1.968	2.126	2.216	2.277	2.276	2.358	2.381	2.439	3.116
r(C2···Cγ) [Å]	3.615	2.544	2.534	2.490	2.369	2.272	2.191	2.171	2.053	2.002	1.891	1.566
V_1(C1,C2)	2.86	2.75	2.74	2.72	2.62	2.52	2.43	2.41	2.30	2.27	2.21	2.08
V_2(C1,C2')	2.73	2.83	2.77	2.74	2.62	2.53	2.46	2.44	2.39	2.38	2.35	2.28
V(C2,C3)	2.87	2.77	2.73	2.71	2.56	2.46	2.38	2.36	2.27	2.23	2.16	2.02
V_1(C2',C3')	} 2.98	} 2.95	} 3.02	} 3.05	} 3.15	} 3.20	} 3.23	} 3.24	} 3.26	} 3.27	1.64	1.58
V_2(C2',C3')											1.66	1.77
V_1(C3,C4)	} 2.90	} 2.92	} 2.98	} 3.02	} 3.12	} 3.18	} 3.23	} 3.23	} 3.29	1.66	1.67	1.69
V_2(C3,C4)										1.66	1.70	1.76
V(C3',C4)	2.74	2.68	2.62	2.59	2.48	2.43	2.38	2.37	2.33	2.31	2.27	2.20
V(C1,O)	1.47	1.54	1.59	1.63	1.77	1.88	1.97	2.00	2.11	2.15	2.21	2.31
V(Cα)	-	0.11	-	-	-	-	-	-	-	-	-	-
V(Cα,O)	1.32	-	-	-	-	-	-	-	-	-	-	-
V_1(Cα,Cβ)	} 2.03	} 2.31	} 2.54	} 2.58	} 2.77	} 3.01	} 3.11	1.48	1.57	1.59	1.63	1.77
V_2(Cα,Cβ)								1.65	1.69	1.70	1.74	1.79
V_1(Cβ,Cγ)	1.77	1.60	1.54	} 3.20	} 3.03	} 2.82	} 2.52	} 2.49	} 2.31	} 2.26	} 2.15	} 1.99
V_2(Cβ,Cγ)	1.78	1.72	1.71									
V(C2)	-	-	-	-	0.13	0.28	0.39	0.41	-	-	-	-
V(C2,Cγ)	-	-	-	-		-	-	-	0.97	1.06	1.27	1.78
V(Cγ)	-	-	-	-		-	0.24	0.27	-	-	-	-
V_1(O)	4.70	2.87	2.84	2.83	2.81	2.79	2.78	2.79	2.75	2.74	2.72	2.67
V_2(O)	-	2.84	2.78	2.76	2.72	2.70	2.69	2.70	2.67	2.66	2.65	2.62
number of attractors	32	32(33)	32	31	32	32	33	34	33	34	35	35

The aromatic ring in APhE is characterized by six valence bonding disynaptic attractors V(C1,C2), V(C2,C3), V(C3,C4), V(C3',C4), V(C2',C3') and V(C1,C2'). There are not observed pairs of the $V_{i=1,2}$(Ci,Cj) attractors that are usually found for localized double C=C bonds [49]. The values of the basin population ($\overline{N}$) are in range from 2.73e for V(C1,C2') to 2.98e for V(C2',C3') yielding the value of ELF-topological bond order for the C-C bonds in the ring between 1.37 and 1.49. Those values are close to formal value of 1.5 expected for benzene. Thus, a delocalized character of valence electron density in the ring has been confirmed. A similar conclusion may be reached on the basis of the values of the relative fluctuation, the quantum-mechanical measure of delocalization of electron density [49–51] that equals 0.47 (λ) for each localization basin representing the C-C bond in the ring (0.46 - benzene [52]).

The formally single bond Cα-Cβ in the side chain –O-Cα-Cβ=Cγ is characterized by the single bonding attractor V(Cα,Cβ) and formally the double bond Cβ=Cγ by pair of the $V_{i=1,2}$(Cβ,Cγ) bonding attractors. Those attractors support the Lewis representation assuming that one attractor corresponds to one bond in the Lewis representation. The double bond Cβ=Cγ "contains" 3.59e (1.77e+1.78e), and that value is slightly (0.41e) smaller than formal value of 4e. The character of the single bond Cα-Cβ is confirmed by population of 2.03e. The C1-O and Cα-O bonds with 1.47 and 1.32e, may be described respectively as the electron depleted single bonds and the „missing" electron density (in respect to a formal value of 2e) is mainly localized in the nonbonding V_1(O) basin. This result suggests a largely polarized character of the carbon – oxygen interaction and its nature may be described by a resonance of three hybrids with the covalent bond, C-O, and the ionic bonds, C^+O^-, C^-O^+ (see Scheme 2).

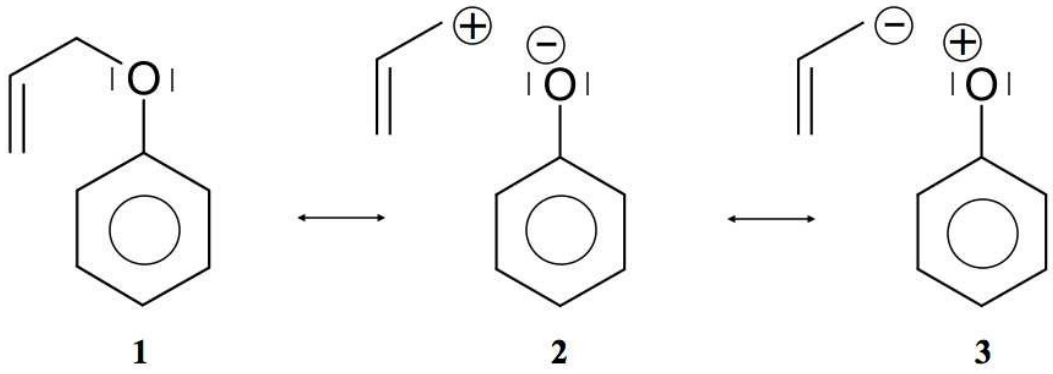

Scheme 2. Three resonance hybrids that describe delocalisation of electron density in the C-O bond in APhE and during the process of dissociation in the steps I and II. The Lewis structures have been drawn on the basis of the results of ELF analysis.

The values of (λ) for the V(C1,O) and V(Cα,O) basins are 0.62 and 0.64, respectively, thus the electron density in those basin are delocalized in a greater degree than for the carbon – carbon bonds in the phenyl ring (0.47). The non-bonding electron density of oxygen is characterized by single valence nonbonding monosynaptic basin $V_1(O)$ with 4.70e. The large value of $\overline{N}$ proves that this basin corresponds to two lone pairs in the Lewis formula.

The product of the reaction, that is ketonic form of o-allylphenol, is formed after migration of the allyl group to orto position of the phenyl ring. All attractors localized in KAPh are presented in Figure 2.

The C2-Cγ bond between the phenyl ring and the allyl group is reflected in ELF-topology by the the V(C2,Cγ) bonding basin. The basin population of V(C2,Cγ) is 1.78e. The Cα-Cβ bond, that is characterized by the single bonding basin V(Cα,Cβ) in APhE is transformed into the double bond Cα=Cβ. The total value of the $\overline{N}$ for two basins $V_1(C\alpha,C\beta)$ and $V_2(C\alpha,C\beta)$ equals 3.56e (1.77e + 1.79e). That value is smaller than formal population of 4e expected for the C=C bond and the "missing" electron density (in respect to a formal value of 4e) is localised in other valence basins. The ketonic form of the o-allylphenol exhibits an essential dearomatisation because for two bonds C2'=C3' and C3=C4 in the phenyl ring two pairs of the disynaptic bonding attractors are found, $V_{i=1,2}(C_2',C_3')$ and $V_{i=1,2}(C_3,C_4)$ with the values of the basin population: 1.58, 1.77e and 1.69e, 1.76e, respectively. The total values of $\overline{N}$ of equaled 3.35e and 3.48e, respectively are about 0.4e larger than corresponding basins in APhE with the aromatic ring. It is worth emphasizing, that the $V_{i=1,2}(C_2',C_3')$ and $V_{i=1,2}(C_3,C_4)$ basins are not observed in APhE before the Claisen rearrangement. Since the Cα-O bond is broken about 0.6e is moved to the region of the non-bonding electron density of oxygen where two non–bonding basins are localized $V_1(O)$, $V_2(O)$ with 2.67e and 2.62e, respectively. The formally double bond C1=O is described by only single V(C1,O) basin with 2.31e, thus similarly to the C1-O and Cα-O bonds in APhE the resonance hybrids with ionic bonds C^+O^-, C^-O^+ have to be considered in description of their electronic structure. It is worth noting that the population of the V(C1,O) basin in KAPh is 0.84e larger than in APhE thus this difference shows that the C1-O bond is saturated with the electron density which may be deduced from comparison of the Lewis formulas (see Scheme 1).

3b. Analysis of reaction mechanism using the DFT (B3LYP) method.

The reaction has been followed by performing the topological analysis of ELF for the 475 nuclear configurations selected along the IRC path (see Figure 3).

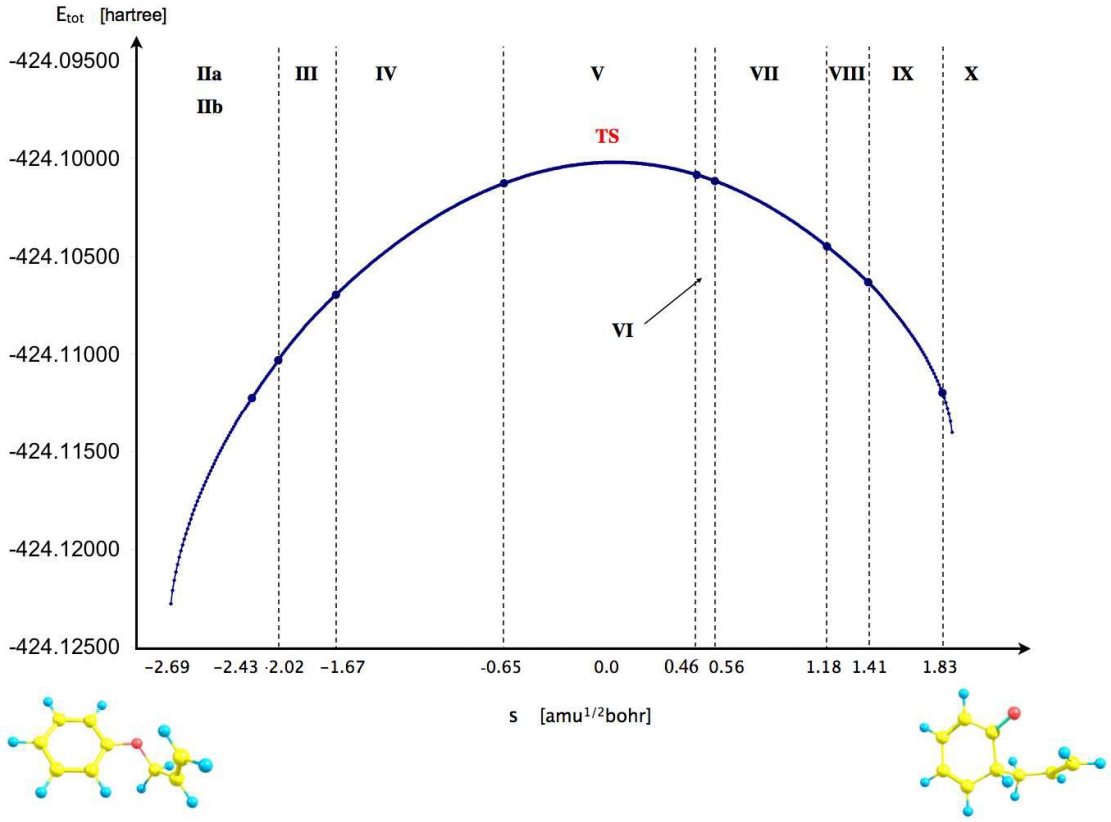

Figure 3. The IRC path calculated for the Claisen rearrangement of the allyl phenyl ether to ketonic form of o-allylphenol with marked domains of structural stability (steps of the reaction) separated by the catastrophes of ELF field.

The values of $\overline{N}$ for the localisation basins observed for an each domain of structural stability - separated by fold and cusp catastrophes of ELF - are showed in Table 1. The Lewis-like structures, representing an evolution of the chemical bonds, lone pairs and non-bonding regions during reaction course are presented in Figure 4.

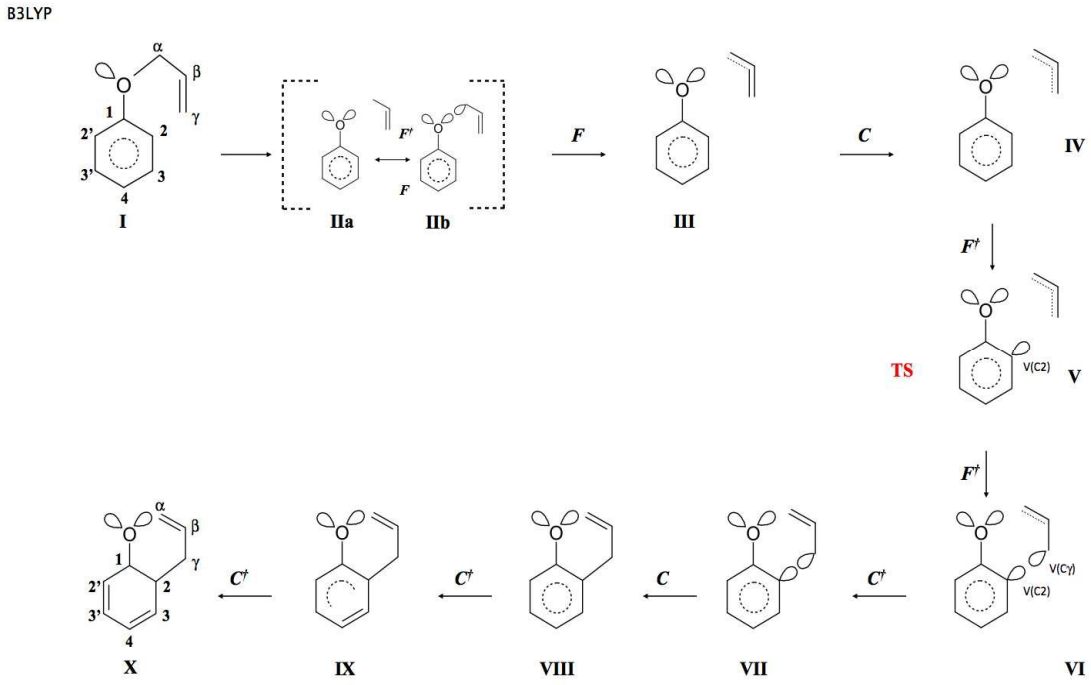

Figure 4. The Lewis-like structures representing the chemical bonds, lone pairs and regions with non-bonding electron density for each step of the Claisen rearrangement of allyl phenyl ether. The results obtained at the DFT(B3LYP)/6-31G(d) computational level. The fold and cusp catastrophes, that cause increase and decrease of the total number of attractors are denoted respectively as: $F^{\dagger}$, $C^{\dagger}$ and F, C.

In the first step of the reaction the topology of the ELF of the reacting molecule is the same as it has been described for the APhE with the geometrical structure optimised to an energy minimum. The number of core and valence attractors equals 32. Among three resonance hybrids showed in Scheme 2 the dominant is hybrid 1.

As a result of the increase of the Cα···O separation an electronic structure of the APhE changes and the weight of the hybrids 2 and 3 increases. The electron density from the Cα-O bond is localised on the Cα or/and O atom. What is interesting, the electronic structure implied by both resonance hybrids is visible in topological analysis of ELF field. The localisation of the electron density on the O atom is represented by second V_2(O) basin localised in the vicinity of the C(O) core basin, while localisation of electron density on the Cα atom is represented by the monosynaptic non-bonding basin V(Cα) localised in the vicinity of the C(Cα) core basin (see modified Lewis structures IIa and IIb in Figure 4). It is worth noting, that the V_2(O) attractor is found in the position where a monosynaptic basin of second lone electron pair of oxygen is expected and not in the bonding region. Thus typical monosynaptic valence attractor, being the remain of the Cα-O bond breaking, that should appear between the C(O) and C(C) core attractors, as showed by Krokidis [14] for the C-C bond

in a process of covalent bond breaking, has not been observed. The synaptic type [53] of the V(Cα) basin is not clear because it may also be disynaptic V(Cα,O). All points on the IRC path up to s = -2.43 $(amu)^{1/2}$ bohr exhibit mainly ELF-topology with the second $V_2(O)$ basin in the valence shell of oxygen (modified Lewis structures IIa). It shows that local electronic structure of the carbon – oxygen bond in a process of its cleavage is dominated by the resonance hybrid 2. The total number of attractors in the molecule does not change in respect to the APhE with the geometrical structure optimised to an energy minimum and equals 32. For larger values of the Cα···O separation the weight of the resonance hybrid 3 increases and some part of electron density from the Cα-O bond is also localised in the vicinity of the C(Cα) core. In addition to the $V_2(O)$ basin the analysis of ELF-topology shows the monosynaptic non-bonding basin V(Cα). The total number of attractors increases to 33 (see modified Lewis structure IIb). We comply with an interpretation that breaking of the Cα-O bond has a complicated mechanism and at early stage of its dissociation an electron density is fluctuating between Cα and O atoms.

The change of the topology of ELF between I and II step is complicated, because it is the result of two processes: a flow of the electron density from the V(Cα,O) basin to a region of the $V_1(O)$ basin and a redistribution of the electron density to a vicinity of the C(Cα) core basin. Both processes are observed in step I. At least three fold catastrophes of the ELF field between steps I and II may be observed. The new valence attractor $V_2(O)$ in a vicinity of the oxygen core C(O) appears in the fold (F^+). The increase of the electron density in the non-bonding region of the O atom results in the qualitative change of electron localisation and the isolation of second local maximum of the ELF, the $V_2(O)$ that corresponds to second lone pair in the formal Lewis representation of the oxygen atom. The $V_2(O)$ attractor corresponds to the lone pair of oxygen (see Figure 4) thus some electron density has been transferred from the bonding to nonbonding region of the oxygen. The decrease of electron density in the Cα-O bond and change of electron localisation may be associated with another fold catastrophe (F) that would describe an annihilation of the bonding attractor. The third fold catastrophe (F^+) results in the appearance of the V(Cα) attractor (or the V(Cα,O) attractor). Unfortunately, a comprehensive description of the Cα-O bond rupture with a verification of the synaptic type of V(Cα) and full characterisation of catastrophes requires a detailed study of all critical points of the ELF field, as presented by Krokidis *et al.* [14] for dissociation of the H_3N-BH_3 molecule. Owing to a complexity of the ELF field in the APhE such analysis can not be performed presently. In Table 1 the basin formed in the vicinity of the C(Cα) core is denoted as the V(Cα) and such abbreviation will be used in the text.

From chemical point of view the covalent-polarized Cα-O bond in step II is partially broken. The basin population of V_2(O) equals 2.84e and is very similar to the one computed for the V_1(O) lone pair with 2.87e. The basin population of the V(Cα) ranges between 0.11÷0.13e. It is worth noting, that very small value of the $\overline{N}$ for the V(Cα) may be explained by small weight of the resonance hybrid 3 where the negative charge is localised on the carbon. The further lengthening of the Cα---O separation results in a redistribution of electron density mainly from the V(Cα) basin to the Cα-Cβ bond. Because of fluctuating electron density between the Cα and O atoms in step II it is not possible to discuss precisely the bond lengths associated with the catastrophes.

Third step (III) of the reaction starts for s = -2.019 $(amu)^{1/2}$ bohr with the fold catastrophe (F). The monosynaptic non-bonding attractor V(Cα) and the CP of index 1 are annihilated and a wandering point i.e. a point at which gradient of ELF does not equal 0 is created. The valence non-bonding basin V(Cα) disappears as a consequence of an electron flow to neighbouring $V_{i=1,2}$(Cα,Cβ) basins and a change of electron localization in the vicinity of the Cα core. The basin population of $V_{i=1,2}$(Cα,Cβ) increases from 2.31 (II) to 2.54e (III). From the beginning of the reaction (step II) the population of both lone pairs V_1(O) and V_2(O) gradually decreases because the electron density flows to the V(C1,O) basin (the double C1=O bond in KAPh). Bearing in mind that the V(Cα) basin in step II was the remain of the Cα-O bond the annihilation of the V(Cα) in step III proves (from ELF-topological point of view) that the Cα-O bond in step III is entirely destroyed.

Step IV of the reaction starts with the cusp catastrophe (C) observed in the region of the Cβ=Cγ bond of the allyl group. Two attractors $V_{i=1,2}$(Cβ,Cγ) and the CP of index 1 are annihilated and a new single attractor V(Cβ,Cγ) appears. Two bonding disynaptic basins $V_{i=1,2}$(Cβ,Cγ) are joined into a single basin V(Cβ,Cγ). Because two attractors $V_{i=1,2}$(Cβ,Cγ) are typical feature of localized double C=C bond therefore observed change of the ELF field may be interpreted as "reduction" of the double Cβ=Cγ bond to the single Cβ-Cγ. The change of the ELF-topology is a consequence of transfer of the electron density mainly from valence basins in the allyl group to a region where the C2-Cγ bond will be formed and from the Cβ=Cγ to Cα-Cβ bond. The mean electron population of the V(Cβ,Cγ) basin equals 3.20e. The catastrophe is found for s = -1.669 $(amu)^{1/2}$ bohr and r(O···Cα) and r(C2···Cγ) distances equal 1.968 Å and 2.490 Å, respectively. In this step all chemical bonds are topologically described by single valence bonding attractors.

The topology of the ELF in a step V is determined by next fold catastrophe (F^+) observed for s= -0.649 $(amu)^{1/2}$ bohr and r(O···Cα) and r(C2···Cγ) distances: 2.126 Å and 2.369 Å, respectively. From the point of view of interpretation of the mechanism of Claisen rearrangement this step is very important because it characterizes the transition state (TS). Valence and core attractors are presented in Figure 2. It is worth to emphasize, that new bond C2-Cγ is not yet formed in the TS, however a progress of the reaction is reflected by formation of new monosynaptic valence basin V(C2) in the vicinity of the C2 core. The V(C2) basin will be transformed into the C2-Cγ bond in the step VIII. The catastrophe "separating" a step IV from a step V is fold. The basin population of $V(C_2)$ equals 0.28e in the TS and during a step V increases from 0.13 to about 0.39e in step VI (see Table 2). All chemical bonds are characterized by single basins with the largest values of $\overline{N}$ calculated for $V_{1\cup2}$(C2',C3'), $V_{1\cup2}$(C3,C4) and V(Cα,Cβ) with 3.20, 3.18 and 3.01e, respectively. Those basins will be transformed into the double bonds.

The sixth step is very short (about 11 points on the IRC path) and begins with the fold (F^+) catastrophe (s = 0.464 $(amu)^{1/2}$ bohr). The non-bonding valence attractor V(Cγ) and CP of index 1 are created in the valence shell of the terminal carbon atom Cγ of the -Cα-Cβ = Cγ allyl group. The total number of attractors increases to 33. The topology of ELF between the C2 and Cγ atoms is characterized by the $V(C_2)$ and V(Cγ) non-bonding attractors. We can say - applying a language of engineering - that "construction" of the C2-Cγ bond is in a very advanced step (see Figure 4). The mean electron population of the $V(C_2)$ and the V(Cγ) basins equals 0.39 and 0.24e, respectively. The formation of the V(Cγ) basin causes large decrease of the population of the V(Cβ,Cγ) basin from 2.82e (TS) to 2.52e (step VI). The values of the r(O···Cα) and r(C2···Cγ) distances for the first point in this step are: 2.277 Å and 2.191 Å, respectively.

A seventh step is associated with a change of an electron localization in the allyl group where the cusp catastrophe (C^+), identified for s ≈ 0.564 $(amu)^{1/2}$ bohr, leads to creation of the critical point of index 1 and two new disynaptic attractors V_1(Cα,Cβ) and V_2(Cα,Cβ) from the single disynaptic attractor V(Cα,Cβ). The total number of attractors increases to 34. The cusp occurs for the r(O···Cα) and r(C2···Cγ) distances equaled 2.276 Å and 2.171 Å. From chemical point of view, the single-type Cα-Cβ bond is transformed into the double Cα=Cβ bond, assuming that a localization of two bonding disynaptic attractors $V_{i=1,2}$(Cα,Cβ) is a typical feature of localized double carbon - carbon bonds. The formation of the Cα=Cβ bond is expected on the basis of a general mechanism of the Claisen rearrangement of APhE. It is

worth to emphasize that emergence of typical feature of the C=C bond occurs before formation of the new C2-Cγ bond that binds the phenyl ring and allyl group. After the catastrophe the values of the basin population of V_1(Cα,Cβ) and V_2(Cα,Cβ) are 1.48e and 1.65e, respectively. A process of their saturation, through steps VIII÷X, continues until maximum values of 1.77e and 1.79e obtained for the KAPh molecule (see Table 1).

A formation of the C2-Cγ bond, between the phenyl and allyl groups, is observed in the step VIII for the r(O···Cα) and r(C2···Cγ) distances equaled 2.358 Å and 2.053 Å, respectively and reaction coordinates s = 1.182 $(amu)^{1/2}$ bohr. In the cusp catastrophe (C) two valence attractors associated with the monosynaptic basins V(C2), V(Cγ) and single CP of index 1 are annihilated yielding new attractor V(C2,Cγ). The number of attractors decreases to 33. From the chemical point of view the observed rearrangement of the ELF-basins is very important – it is evident, that the covalent bond between the C2 and Cγ atoms has been formed. Thus, the allyl group and phenyl ring has been "put together". After the cusp the basin population of V(C2,Cγ) equals 0.97e and increases to 1.06e and 1.27e in the steps IX and X, respectively with maximum of 1.78e for KAPh with geometrical structure optimized to energy minimum.

Two last steps, IX and X, characterize a formation of two double bonds C3=C4, C2'=C3' in initially fully aromatic phenyl ring. It is worth noting, that signs of dearomatisation of the phenyl ring - visible in topology of ELF - are observed just at the end of the Claisen rearrangement. The electron density delocalized in the phenyl ring is concentrated in the C3=C4 and C2'=C3' bonds and this process is associated with a local change of the electron localization and finally with the change of the ELF-topology. Two catastrophes of the cusp type (C^+) are observed for s = 1.409 (IX) and 1.827 (X) $(amu)^{1/2}$ bohr that corresponds to the r(O···Cα) and r(C2···Cγ) distances equaled 2.381, 2.002Å and 2.439, 1.891Å, respectively. The double bond C3=C4 exhibits topology of the ELF with two bonding basins $V_{i=1,2}$(C3,C4) for 1.361Å and the C2'=C3' bond with two $V_{i=1,2}$(C2',C3') basins for 1.359 Å, thus both bond lengths are very similar. It is also worth noting, that first in a step IX the $V_{i=1,2}$(C3,C4) basins are formed for the bond that is separated by only one single C2-C3 bond from the allyl group. The C2'=C3' bond is formed in the last step X and that bond is separated from the allyl group by two single bonds C1-C2 and C1-C2'. Dearomatisation of the ring results from the electron density redistribution which proceeds (see Scheme 3) mainly from the C1-C2', C3'-C4 and C2-C3 bonds. The value of the basin population for newly created C3=C4 bond is 1.66e (both basins) and of the C2'=C3' are 1.64e (V_1(C2',C3')) and 1.66e (V_2(C2',C3')).

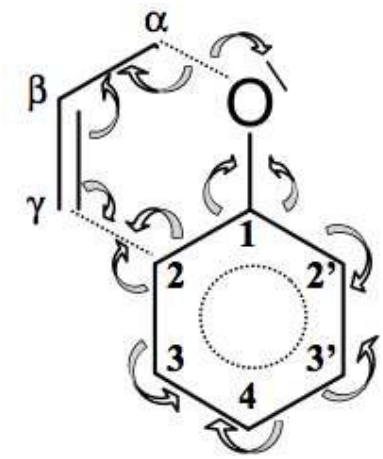

Scheme 3. Redistribution of electron density during Claisen rearrangement of allyl phenyl ether obtained from topological analysis of ELF.

From the perspective of ELF-analysis the formation of the product of the Claisen reaction of APhE, that is ketonic form of o-allylphenol, has been terminated in step X. The Lewis-like formula for the KAPh, obtained on the basis of topology of the ELF (see Figure 4), is very similar to the Lewis structure drawn on the basis of assumption that carbon and oxygen atoms achieve a valence shell electron configuration with a full octet of electrons and hydrogen with doublet of electrons. The difference is found for the carbon – oxygen bond that is formally represented by the double C=O bond, meanwhile topological analysis of the ELF exhibits only the one V(C1,O) attractor and basin. Thus, the carbon - oxygen bond is much polar than suggested by the Lewis structure and at least three resonance hybrids should be used: C-O, $C^{+}O^{-}$ and $C^{-}O^{+}$. In effect the C-O bond in step X (see Figure 4) is represented only by single line. In the valence space of the oxygen atom two non-bonding basins of oxygen, $V_1(O)$ and $V_2(O)$ are observed with and total basin population of 5.29e.

3c. Analysis of reaction mechanism using the DFT (M052x) method.

The changing location of the $V_2(O)$ and V(Cα) attractors, observed for the points on the IRC path in step II, may be related to the electron density functional and the basis set used in the calculations. Therefore, an analysis has been repeated using the DFT (M052x) method and 6-311G(d) basis set. 459 points on the IRC path, from the TS towards the substrate (APhE), have been analyzed with step of 0.01 $(amu)^{1/2}$ bohr. The analysis of ELF for the isolated APhE molecule shows different topology than obtained using DFT (B3LYP) method.

In the region of non-bonding electron density of oxygen two monosynaptic non-bonding basins $V_{i=1,2}(O)$ have been localised with the population equalled 2.35 and 2.50e. Two non-bonding basins and two bonding basins, V(C1,O) and V(Cα,O), associated with the oxygen atom correspond to the sp^3 hybridisation of atomic orbitals and support the Lewis structure of APhE. The electronic structure of TS is very similar to that obtained using the B3LYP functional with characteristic non-bonding attractor V(C2) with the basin population 0.25e.

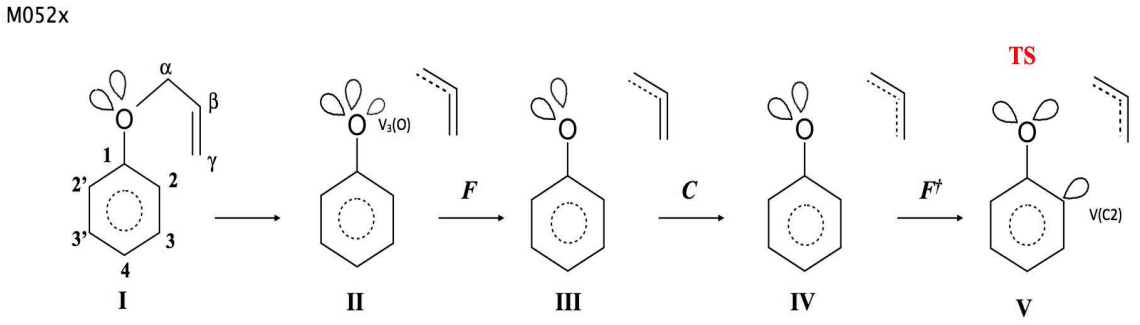

Figure 5. The Lewis-like structures representing the chemical bonds, lone pairs and regions with non-bonding electron density for five steps of the Claisen rearrangement of allyl phenyl ether. The results obtained at the DFT(M052x)/6-311G(d) computational level.

The picture of the Cα-O bond's dissociation is less complicated than obtained using the DFT (B3LYP) method. The topological analysis of ELF, performed for the points on the IRC path, shows five domains of structural stability (see Figure 5). The structures IIa and IIb, which reflect delocalisation of the bonding pair between the Cα and O atoms (B3LYP), have not been observed. The heterolytic cleavage of the Cα-O bond is characterised in step I by annihilation of the disynaptic V(Cα,O) attractor and appearance of new monosynaptic attractor $V_3(O)$. Unfortunately, the change of topology of ELF associated with the bond lengthening is complicated hence exact position and type of the catastrophe on the IRC path could not be obtained. It is worth noting, that the $V_3(O)$ basin is localised between the C(Cα) and C(O) core basins, and not in the position of the $V_2(O)$ attractor, as it was showed by the analysis using the B3LYP functional. This issue suggests that both computational methods exhibit different details of evolution of the electronic structure of the Cα-O bond. The $V_3(O)$ attractor is annihilated in step III for the Cα···O distance equalled 1.816Å. The non-bonding attractor V(C2), that reflects the beginning of formation of the C2-Cγ bond, is observed for TS for the C2···Cγ distance equalled 2.159Å. The analysis of the DFT (M052x) data supports and complements the description of the mechanism of the C-O bond breaking obtained using DFT (B3LYP) method. However, it should be considered, that the number and synaptic type

as well as localisation in space of valence basins associated with the C-O bond breaking may depend on used DFT functional.

4. Conclusions

The application of Bonding Evolution Theory for the DFT (B3LYP) and DFT (M052x) data allowed explaining precisely the mechanism of the Claisen rearrangement of the allyl phenyl ether in a real space without using a concept of molecular orbital in the Hilbert space. The process of a bond breaking and a bond formation during transformation of the APhE to the KAPh has been clearly characterized.

The reaction consists of 10 main steps (B3LYP) and an each step may be characterized as follows: at first the chemical bond Cα-O is broken (step IIa, IIb), the remain of the Cα-O bond, that is the non-bonding V(Cα) basin, is annihilated as a result of a transfer of the electron density to the Cα-Cβ bond (step III), the double bond Cβ=Cγ in the allyl group is "reduced" to the single bond Cβ-Cγ as a result of a transfer of the electron density to the Cα-Cβ and C2···Cγ regions (step IV), starts the "construction" of the C2-Cγ bond between the allyl group and the phenyl ring through the formation of the V(C2) basin (step V), the "construction" of the C2-Cγ bond continues through the formation of the second V(Cγ) basin (step VI), the double bond Cα=Cβ in the allyl group is formed (step VII), the C2-Cγ bond between the allyl group and the phenyl ring is formed (step VIII), the first stage of the dearomatisation of the phenyl ring starts through the formation of localized the C3-C4 bond (step IX), the dearomatisation of the phenyl ring continues through the formation of the second localized the C2'-C3' bond in the phenyl ring and this step ends the Claisen rearrangement of the APhE. The BET analysis performed for the M052x data (IRC from TS to APhE) also shows five steps of the reaction and very similar topology of ELF for TS.

The breaking of the carbon-oxygen bond from the ELF-perspective is a complicated process that depends on the DFT functional used. For a number of points on the IRC path the DFT (B3LYP) calculations show the fluctuating electron density between C and O atoms (started in a step I and clearly visible in a step II). Such mechanism seems to be correctly represented by two formal resonance hybrids with heterolytically broken bond, $C^{+}O^{-}$, $C^{-}O^{+}$. The application of the M052x functional yields simpler picture where the breaking of the C-O bond causes the formation of the non-bonding monosynaptic basin $V_3(O)$. Those results show that the choice of the DFT functional may be crucial for qualitative description of the breaking of the carbon-oxygen bond.

Finally, we may answer the questions posed at the beginning of our paper. **1)** The redistribution of the electron density in the APhE is not as simple as usually depicted (see Scheme 1). A formation of new bond requires a supply of the electron density, usually from neighbouring bonds, thus a picture of the electron flow is much complicated (see Scheme 3). **2)** Given that the term "synchronous mechanism" refers to a breaking and formation of the chemical bonds in the same moment of the reaction path (for instance in the TS), our study shows that in the case of the Claisen rearrangement of the APhE the mechanism is asynchronous. In the transition structure (step V) the new C2-Cγ bond between the allyl group and the phenyl ring is not yet formed but the Cα-O bond is already entirely broken (step III). The process of a concentration of the electron density in the C2···Cγ region continues and in the vicinity of the Cα core a degree of the electron localization is high enough to observe the local attractor V(Cα) and its basin. **3)** The double C=C bonds in the six–membered ring are formed in the final steps of the reaction after the Cα-O bond is broken, the C=C bond in the allyl group is translated to other position and the C2-Cγ bond is formed.

The presented picture of the evolution of the chemical bonds in the Claisen rearrangement of the APhE rules out the pericyclic mechanism, because the electron density flow does not take place in a cyclic, one-way curve. In this context it is worth to mention the recent study by Domingo [54,55] who also refuted the pericyclic mechanism for the Diels-Alder reaction between ethylene and butadiene.

Acknowledgments

The authors would like acknowledge to gratefully the Wroclaw Centre for Networking and Supercomputing (WCSS) for the allocation of computer time on the **BEM** Cluster and also the Academic Computer Centre in Gdańsk (CI TASK) for the allocation of computer time on the **Tryton** Cluster. The Marie Curie European Reintegration Grant supported the work of S.B. – contract N^{o} MERG-CT-2004-006330. "The authors are solely responsible for the information communicated and it does not represent the opinion of The European Community. The European Community is not responsible for any use that might be made of data appearing therein". Special thanks to Piotr Skoluda for editing this document.

5. References

1 A. M. Martin Castro, *Chem. Rev.*, 2014, **104**, 2939.

2 L. Claisen, *Chem. Ber.* 1912, **45**, 3157.

3 A. D. Becke, K. E. Edgecombe, *J. Chem. Phys.*, 1990, **92**, 5397.

4 B. Silvi, A. Savin, *Nature*, 1994, **371**, 683.

5 A. Savin, B. Silvi, F. Colonna, *Can. J. Chem.*, 1996, **74**, 1088.

6 B. Silvi, *J. Mol. Struct.*, 2002, **614**, 3.

7 A. Savin, *J. Mol. Struct. THEOCHEM*, 2005, **727**, 127.

8 A. Savin, J. Chem. Sci., 2005, **117**, 473.

9 R. Thom, *Stabilité Structurelle et Morphogénèse*, InterEditions, Paris, 1972.

10 D. Roca–López, V. Polo, T. Tejero, P. Merino, *Eur. J. Org. Chem.*, 2015, **2015**, 4143.

11 D. Roca–López, V. Polo, T. Tejero, P. Merino, *J. Org. Chem.*, 2015, **80**, 4076.

12 V. Polo, J. Andrés, *J. Comput. Chem.*, 2005, **26**, 1427.

13 I. M. Ndassa, B. Silvi, F. Volatron, *J. Phys. Chem. A*, 2010, **114**, 12900.

14 X. Krokidis, S. Noury, B. Silvi, *J. Phys. Chem. A*, 1997, **101**, 7277.

15 X. Krokidis, B. Silvi, M. E. Alikhani, *Chem. Phys. Lett.*, 1998, **292**, 35.

16 X. Krokidis, B. Silvi, C. Dezarnaud–Dandine, A. Sevin, *New J. Chem.*, 1998, **22**, 1341.

17 X. Krokidis, R. Vuilleumier, D. Borgis, B. Silvi, *Mol. Phys.*, 1999, **96**, 265.

18 S. Yamabe, S. Okumoto, T. Hayashi, *J. Org. Chem.*, 1996, **61**, 6218.

19 O. Wiest, K. A. Black, K. N. Houk, *J. Am. Chem. Soc.*, 1994, **116**, 10336.

20 M. J. S. Dewar, C. Jie, *J. Am. Chem. Soc.*, 1989, **111**, 511.

21 M. M. Davidson, I. H. Hillier, M. A. Vincent, *Chem. Phys. Lett.*, 1995, **246**, 536.

22 H. Y. Yoo, K. N. Houk, *J. Am. Chem. Soc.*, 1994, **116**, 12047.

23 M. P. Meyer, A. J. DelMonte, D. A. Singleton, *J. Am. Chem. Soc.*, 1999, **121**, 10865.

24 Gaussian 03, Revision C.02, M. J. Frisch, G. W. Trucks, H. B. Schlegel, G. E. Scuseria, M. A. Robb, J. R. Cheeseman, J. A. Montgomery, Jr., T. Vreven, K. N. Kudin, J. C. Burant, J. M. Millam, S. S. Iyengar, J. Tomasi, V. Barone, B. Mennucci, M. Cossi, G. Scalmani, N. Rega, G. A. Petersson, H. Nakatsuji, M. Hada, M. Ehara, K. Toyota, R. Fukuda, J. Hasegawa, M. Ishida, T. Nakajima, Y. Honda, O. Kitao, H. Nakai, M. Klene, X. Li, J. E. Knox, H. P. Hratchian, J. B. Cross, V. Bakken, C. Adamo, J. Jaramillo, R. Gomperts, R. E. Stratmann, O. Yazyev, A. J. Austin, R. Cammi, C. Pomelli, J. W. Ochterski, P. Y. Ayala, K. Morokuma, G. A. Voth, P. Salvador, J. J. Dannenberg, V. G. Zakrzewski, S. Dapprich, A. D. Daniels, M. C. Strain, O. Farkas, D. K. Malick, A. D. Rabuck, K. Raghavachari, J. B. Foresman, J. V. Ortiz, Q. Cui, A. G. Baboul, S. Clifford, J. Cioslowski, B. B. Stefanov, G. Liu, A. Liashenko, P. Piskorz, I. Komaromi, R. L. Martin, D. J. Fox, T. Keith, M. A. Al-Laham, C. Y. Peng, A.

Nanayakkara, M. Challacombe, P. M. W. Gill, B. Johnson, W. Chen, M. W. Wong, C. Gonzalez, and J. A. Pople, Gaussian, Inc., Wallingford CT, 2004.

25 A. D. Becke, *J. Chem. Phys.*, 1993, **98**, 5648.

26 P. J. Stephens, F. J. Devlin, C. F. Chabalowski, M. J. Frisch, J. Phys. Chem., 1994, **98**, 11623.

27 K. Kim, K. D. Jordan, *J. Phys. Chem.*, 1994, **98**, 10089.

28 C. Lee, W. Yang, R. G. Parr, *Phys. Rev. B*, 1988, **37**, 785.

29 R. Ditchfield, W. J. Hehre, J. A. Pople, *J. Chem. Phys.*, 1971, **54**, 724.

30 W. J. Hehre, R. Ditchfield, J. A. Pople, *J. Chem. Phys.*, 1972, **56**, 2257.

31 C. Hariharan, J. A. Pople, *Theor. Chem. Acc.*, 1973, **28**, 213.

32 P. C. Hariharan, J. A. Pople, *Mol. Phys.*, 1974, **27**, 209.

33 M. S. Gordon, *Chem. Phys. Lett.*, 1980, **76**, 163.

34 M. M. Francl, W. J. Pietro, W. J. Hehre, J. S. Binkley, D. J. DeFrees, J. A. Pople, M. S. Gordon, *J. Chem. Phys.*, 1982, **77**, 3654.

35 R. C. Binning Jr., L. A. Curtiss, *J. Comp. Chem.*, 1990, **11**, 1206.

36 J. -P. Blaudeau, M. P. McGrath, L. A. Curtiss, L. Radom, *J. Chem. Phys.*, 1997, **107**, 5016.

37 V. A. Rassolov, J. A. Pople, M. A. Ratner, T. L. Windus, *J. Chem. Phys.*, 1998, **109**, 1223.

38 V. A. Rassolov, M. A. Ratner, J. A. Pople, P. C. Redfern, L. A. Curtiss, *J. Comp. Chem.*, 2001, **22**, 976.

39 G. A. Petersson, A. Bennett, T. G. Tensfeldt, M. A. Al-Laham, W. A. Shirley, J. Mantzaris, *J. Chem. Phys.*, 1988, **89**, 2193.

40 G. A. Petersson, M. A. Al-Laham, *J. Chem. Phys.*, 1991, **94**, 6081.

41 Y. Zhao, N. E. Schultz, D. G. Truhlar, *J. Chem. Theory Comput.*, 2006, **2,** 364.

42 Gaussian 09, Revision E.01, M. J. Frisch, G. W. Trucks, H. B. Schlegel, G. E. Scuseria, M. A. Robb, J. R. Cheeseman, G. Scalmani, V. Barone, B. Mennucci, G. A. Petersson, H. Nakatsuji, M. Caricato, X. Li, H. P. Hratchian, A. F. Izmaylov, J. Bloino, G. Zheng, J. L. Sonnenberg, M. Hada, M. Ehara, K. Toyota, R. Fukuda, J. Hasegawa, M. Ishida, T. Nakajima, Y. Honda, O. Kitao, H. Nakai, T. Vreven, J. A. Montgomery, Jr., J. E. Peralta, F. Ogliaro, M. Bearpark, J. J. Heyd, E. Brothers, K. N. Kudin, V. N. Staroverov, R. Kobayashi, J. Normand, K. Raghavachari, A. Rendell, J. C. Burant, S. S. Iyengar, J. Tomasi, M. Cossi, N. Rega, J. M. Millam, M. Klene, J. E. Knox, J. B. Cross, V. Bakken, C. Adamo, J. Jaramillo, R. Gomperts, R. E. Stratmann, O. Yazyev, A. J. Austin, R. Cammi, C. Pomelli, J. W. Ochterski, R. L. Martin, K. Morokuma, V. G. Zakrzewski, G. A. Voth, P. Salvador, J. J. Dannenberg, S.

Dapprich, A. D. Daniels, Ö. Farkas, J. B. Foresman, J. V. Ortiz, J. Cioslowski, and D. J. Fox, Gaussian, Inc., Wallingford CT, 2009.

43 R. Krishnan, J. S. Binkley, R. Seeger, J. A. Pople, *J. Chem. Phys.*, 1980, **72**, 650.

44 K. Fukui, *J. Phys. Chem.*, 1970, **74**, 4161.

45 K. Fukui, *Acc. Chem. Res.*, 1981, **14**, 363.

46 S. Noury, X. Krokidis, F. Fuster, B. Silvi, *Comput. Chem.*, 1999, **23**, 597.

47 ChemCraft, version 1.7, G. A. Andrienko, http://www.chemcraftprog.com.

48 B. Gómez, P. K. Chattaraj, E. Chamorro, R. Contreras, P. Fuentealba, *J. Phys. Chem. A*, 2002, **106**, 112227.

49 A. Savin, B. Silvi, F. Colonna, *Can. J. Chem.*, 1996, **74**, 1088.

50 S. Noury, F. Colonna, A. Savin, B. Silvi, *J. Mol. Struct.*, 1998, **450**, 59.

51 B. Silvi, *Phys. Chem. Chem. Phys.*, 2004, **6**, 256.

52 S. Noury, F. Colonna, A. Savin, B. Silvi, *J. Mol. Struct.*, 1998, **450**, 59.

53 B. Silvi, *J. Mol. Struct.*, 2002, **614**, 3.

54 L. R. Domingo, *Org. Chem. Curr. Res.*, 2013, **2**, 120.

55 L. R. Domingo, *RSC Adv.*, 2014, **4**, 32415.

A mechanism of the Claisen rearrangement of allyl phenyl ether was studied by means of BET and ELF. We have showed the mechanism of reaction as a sequence of a bond breaking and a bond formation that are precisely located on the reaction path by means of catastrophe theory.